**The EMBO Journal** Vol. 21 No. 9 pp. 2095–2106, 2002

# The complex of Arl2-GTP and PDEδ: from structure to function

**Michael Hanzal-Bayer[1], Louis Renault[1,2], Pietro Roversi[3], Alfred Wittinghofer[1,4] and Roman C.Hillig[1,4,5]**

[1]Max-Planck-Institut für molekulare Physiologie, Abteilung Strukturelle Biologie, Otto-Hahn-Strasse 11, D-44227 Dortmund, Germany and [3]GlobalPhasing Ltd, Sheraton House, Castle Park, Cambridge CB3 0AX, UK

[2]Present address: Laboratoire d'Enzymologie et Biochimie Structurales, CNRS, Avenue de la Terrasse, F-91198 Gif-sur-Yvette, France
[5]Present address: Schering AG Research Laboratories, D-13342 Berlin, Germany

[4]Corresponding authors
e-mail: alfred.wittinghofer@mpi-dortmund.mpg.de or roman.hillig@schering.de

**Arf-like (Arl) proteins are close relatives of the Arf regulators of vesicular transport, but their function is unknown. Here, we present the crystal structure of full-length Arl2-GTP in complex with its effector PDEδ solved in two crystal forms (Protein Data Bank codes 1KSG, 1KSH and 1KSJ). Arl2 shows a dramatic conformational change from the GDP-bound form, which suggests that it is reversibly membrane associated. PDEδ is structurally closely related to RhoGDI and contains a deep empty hydrophobic pocket. Further experiments show that H-Ras, Rheb, Rho6 and $G\alpha_{i1}$ interact with PDEδ and that, at least for H-Ras, the intact C-terminus is required. We suggest PDEδ to be a specific soluble transport factor for certain prenylated proteins and Arl2-GTP a regulator of PDEδ-mediated transport.**

*Keywords*: Arf-like proteins/GDI/phosphodiesterase 6D/Ras/transport

## Introduction

Guanine nucleotide binding proteins (GNBPs) of the Ras superfamily are involved in the regulation of a wide variety of cellular processes and act as molecular switches cycling between an inactive GDP-bound and an active GTP-bound state. The superfamily consists of five established subfamilies, where each subfamily member regulates a similar process. Members of the ADP-ribosylation factor (Arf) subfamily are regulators of vesicle formation in intracellular traffic that interact reversibly with membranes of the secretory and endocytic compartments in a GTP-dependent manner (Chavrier and Goud, 1999).

Arf proteins are believed to be recruited to a specific membrane by a corresponding Arf-specific guanine nucleotide exchange factor (GEF). After GDP–GTP exchange, GTP-bound Arf is involved in recruiting components of the vesicular coat and the proper cargo. Vesicle formation is terminated by Arf-mediated GTP hydrolysis, which is accelerated by Arf-specific GTPase-activating proteins (GAPs). Biochemical studies (Franco *et al*., 1996; Antonny *et al*., 1997) and various crystal structures (Amor *et al*., 1994; Greasley *et al*., 1995; Goldberg, 1998; Menetrey *et al*., 2000; Amor *et al*., 2001; Pasqualato *et al*., 2001) have revealed that Arf proteins undergo a so-called β-sheet register shift between the GDP and the GTP conformation that promotes the release of an Arf-specific N-terminal myristoylated α-helix.

In addition to Arfs, the Arf subfamily contains another, more heterogenous group of proteins with hitherto unknown function. These Arf-like (Arl) proteins (Tamkun *et al*., 1991) are similar in sequence but do not complement the lethal *Saccharomyces cerevisiae* double mutant *arf1*$^-$ *arf2*$^-$. They neither act as co-factors in the cholera toxin (CTA) catalyzed ADP-ribosylation of $G\alpha_s$, nor as activators of phospholipase D (PLD). The only exception to this rule is Arl1, as it has some co-factor activity in the CTA assay and weakly stimulates PLD activity (Hong *et al*., 1998). Since it shares an identical core effector region with Arf1 and its GTP hydrolysis is sensitive to ArfGAP (Ding *et al*., 1996), it should rather be considered an atypical Arl protein.

We have previously identified murine Arl2 (M.Hanzal-Bayer, manuscript in preparation) and Arl3 (Linari *et al*., 1999) as interaction partners of PDEδ (see below). For Arl2, two additional interacting proteins, the binder of Arl2 (BART) and the tubulin-folding co-factor D have been described (Sharer and Kahn, 1999; Bhamidipati *et al*., 2000). Recently, we reported the structure of Arl3-GDP (Hillig *et al*., 2000) and demonstrated that it is very similar to that of Arf1-GDP (Amor *et al*., 1994; Greasley *et al*., 1995), which was recently confirmed by the structure of Arl1 (Amor *et al*., 2001). Differences between Arf and Arl proteins do, however, exist, since the N-termini of Arl2 and Arl3 could not be myristoylated under conditions suitable for Arf (Cavenagh *et al*., 1994; Randazzo *et al*., 1995; Eboue *et al*., 1998; Sharer and Kahn, 1999; Cuvillier *et al*., 2000), and our structure revealed that the N-terminal region of Arl3-GDP does not fold into a helix. Nevertheless, we postulated that Arl3 would release its N-terminus upon binding to GTP and that its N-terminus may be modified with a myristate derivative, as observed earlier for other 'myristoylated' proteins (Hillig *et al*., 2000).

Human PDEδ was originally identified as a fourth subunit of rod-specific cGMP phosphodiesterase, PDE6 (EC 3.1.4.35) (Gillespie *et al*., 1989; Florio *et al*., 1996). Catalytically active PDE6 is a heterodimer (αβ) that is regulated by two inhibitory γ subunits. As PDEδ does not modify the catalytic properties ($K_M$, $V_{max}$) of PDEαβ (Gillespie *et al*., 1989), its function is still unresolved. It has been suggested, however, that PDEδ can extract PDEαβ from membranes. PDEαβ is a dually modified

protein where PDEα is farnesylated and PDEβ geranylgeranylated (Qin *et al*., 1992). Although PDEαβ can therefore associate tightly with photoreceptor disc membranes, 20–30% of total rod PDEαβ is soluble, and PDEδ is found exclusively associated with the soluble fraction (Gillespie *et al*., 1989; Florio *et al*., 1996; Cook *et al*., 2000). It has been demonstrated that PDEδ binds to either subunit via its processed C-terminus, and that this interaction depends not only on prenylation, but also on tripeptide cleavage and carboxymethylation (Cook *et al*., 2000). In permeabilized rod outer segments, recombinant GST-PDEδ can solubilize endogenous catalytic PDE and thereby decouple cGMP hydrolysis from transducin activation (Cook *et al*., 2001). In epithelial cells, PDEδ can solubilize the small GNBP Rab13 (Marzesco *et al*., 1998). Taken together, these findings suggest that PDEδ can translocate membrane-anchored proteins into the cytosol. Although there is as yet no evidence that membrane localization of PDEαβ is a regulated event *in vivo* (Cook *et al*., 2001), PDEδ would then exert a function reminiscent of that of guanine nucleotide dissociation inhibitors (GDIs), which solubilize Rab and Rho GNBPs (Olofsson, 1999).

In contrast to PDEαβ$\gamma_2$, PDEδ is not confined to photoreceptor cells but is widely distributed in different tissues (Florio *et al*., 1996; Marzesco *et al*., 1998). In addition, a PDEδ homolog in *Caenorhabditis elegans* shares 69% homology with human PDEδ. This is one of the strongest conservations ever observed between these two species (Lorenz *et al*., 1998), and PDEδ from *C.elegans* can also solubilize human PDEαβ (Li and Baehr, 1998), which strongly suggests a more general function of PDEδ. In contrast to its putative GDI-like function, we demonstrated that PDEδ binds to truncated, non-modified Arl2 and Arl3 in a GTP-specific manner, which indicates that, here, PDEδ is an Arl effector and not a GDI. We also observed that PDEδ exhibits a strong inhibitory effect on dissociation of GTP from Arl2 and Arl3 (Linari *et al*., 1999), which is not unusual for an effector (Herrmann *et al*., 1995). In order to obtain further insight into the function of PDEδ, we determined the structure of Arl2-GTP in complex with PDEδ. The unexpected close structural similarity of PDEδ to RhoGDI led us to carry out some additional biochemical experiments to further clarify the role of PDEδ.

## Results

### *Structure determination*

The complex of Arl2 and PDEδ was formed *in vivo* by co-expression of both proteins in *Escherichia coli*, and was subsequently co-purified and crystallized in two crystal forms as described previously (Renault *et al*., 2001). The structure was determined by a combination of molecular replacement and single wavelength anomalous dispersion (SAD) (for statistics, see Table I).

While crystals of form-1 grew within days, those of form-2 crystallized only after several months to 1 year (Renault *et al*., 2001). Whereas the active site of Arl2 in form-1 contains GTP, as expected, the electron density in form-2 suggests partial hydrolysis of GTP to GDP and phosphate, which led us to model the nucleotide as GDP plus phosphate (Figure 1A). Occupancy refinement converges at a ratio of 3:1 for GDP/phosphate:GTP and was confirmed by high-performance liquid chromatography (HPLC) (see Materials and methods). We do not observe any significant differences within Arl2 or at the Arl2:PDEδ interface between the two crystal forms. Overall, form-2 shows a more favorable crystal packing, with PDEδ in particular being much better defined. Whereas the N-terminus of Arl2 is ordered as an α-helix stabilized via crystal contacts in form-1, it is either flexible or not visible due to partial proteolytic degradation in form-2 (see Materials and methods).

### *The structure of Arl2-GTP*

Arl2-GTP in the complex of Arl2-GTP:PDEδ shows the typical G domain fold of Ras proteins with a six-stranded β-sheet surrounded by five α-helices (Figure 1B), with an additional α-helix ($\alpha_0$) at the N-terminus. Although crystal form-2 contains predominantly Arl2-GDP plus phosphate, the switch regions of Arl2 in both forms adopt the conformation characteristic for the GTP-bound form of a small GNBP, with a root mean square deviation (r.m.s.d.) of only 0.7 Å for all but the N-terminal 15 residues. The only deviation concerns residues $Asp40_A$ to $Thr43_A$ in a poorly defined loop region (residues of Arl2 will be designated by a subscript A, those of PDEδ by a subscript P hereafter).

The structures of various full-length Arf proteins in the GDP conformation have been determined previously (see Introduction), whereas GTP-bound structures were missing the N-terminus, either due to truncation (Goldberg, 1998) or disorder in the crystal (Pasqualato *et al*., 2001). Here we show the first defined N-terminus of an Arf subfamily member. As Arl2 is most closely related to Arl3 (53% sequence identity, 63% similarity; Figure 1C) and Arl3 is the only other Arf subfamily protein to interact with PDEδ (M.Hanzal-Bayer, manuscript in preparation), comparison of Arl2-GTP with Arl3-GDP (Hillig *et al*., 2000) allows a detailed description of the conformational changes taking place upon nucleotide exchange (analysis based on crystal form-1). Concluding from the conformational changes observed, and leaving out the interswitch region (Figure 1B), we define switch I as the region comprising residues $Asn37_A$ to $Phe50_A$ (residues 38–51 in Arl3). In the GTP form, the additional β-strand ($\beta_{2E}$) of switch I observed in Arl3-GDP is unfolded to take $Thr47_A$ ($Thr35_{Ras}$) close to the nucleotide, where it plays its canonical role in magnesium and γ phosphate co-ordination. Switch II is formed by residues $Asp66_A$ to $Asn79_A$. The conformational change enables $Gly69_A$ ($Gly60_{Ras}$) of the $^{66}$DxxGQ$^{70}$ motif to adopt its canonical role in the co-ordination of the γ phosphate. As postulated from the structural analysis of Arl3-GDP (Hillig *et al*., 2000), the interswitch region ($Asn51_A$ to $Trp65_A$) has undergone a β-sheet register shift, with β-strands β2 and β3 sliding by two residues relative to the remaining β-sheet (Figure 1B and D). This most remarkable conformational change involves the breakage of hydrogen bonds connecting strands β1 and β3, the movement of the interswitch region and finally the formation of new hydrogen bonds. The shift of the interswitch region results in the displacement of the N-terminus, which changes its conformation from the extended loop with just a single helical turn observed in Arl3-GDP to an amphipathic

**Table I.** Data collection and refinement statistics

| Data set | Native-1 (crystal form-1) | Native-2 (crystal form-2) | SeMet (crystal form-2) |
|---|---|---|---|
| Data collection[a] | | | |
| Crystal size (μm$^3$) | 10 × 60 × 300 | 400 × 400 × 400 | 30 × 80 × 100 |
| X-ray source (wavelength in Å) | ESRF ID13 (0.782) | DESY BW6 (1.005) | ESRF ID13 (0.964) |
| Space group | $P2_1$ | $P2_12_12_1$ | $P2_12_12_1$ |
| Unit cell parameters | *a* = 48.1 Å, *b* = 45.7 Å, *c* = 74.7 Å, β = 94.0° | *a* = 44.5 Å, *b* = 65.4 Å, *c* = 104.4 Å | *a* = 44.8 Å, *b* = 65.7 Å, *c* = 104.0 Å |
| Mosaicity (°) | 0.45 | 0.61 | 1.20 |
| Resolution range (Å) | 19.7–2.3 | 34.7–1.8 | 19.8–2.6 |
| Highest resolution shell (Å) | 2.35–2.30 | 1.84–1.80 | 2.65–2.60 |
| Unique reflections | 14 251 | 28 815 | 9926 |
| Multiplicity[b] | 2.9 (3.0) | 8.6 (7.9) | 8.7 (9.6) |
| Completeness (%)[b] | 97.5 (99.7) | 99.5 (98.9) | 99.6 (100.0) |
| $R_{symm}$[b,c] | 0.065 (0.235) | 0.042 (0.316) | 0.081 (0.391) |
| $I/\sigma$[b] | 14.8 (5.8) | 38.8 (4.8) | 25.1 (7.0) |
| Refinement | | | |
| Resolution (Å) | 19.7–2.3 | 34.7–1.80 | 19.8–2.6 |
| Highest resolution shell (Å) | 2.44–2.30 | 1.91–1.80 | 2.76–2.60 |
| Reflections (work set/test set) | 12 832/1406 | 24 859/2725 | 8957/953 |
| Non-hydrogen atoms | 2597 | 2696 | 2702 |
| $R_{work}$[b,d] | 0.255 (0.314) | 0.244 (0.413) | 0.209 (0.232) |
| $R_{free}$[b,e] | 0.301 (0.390) | 0.271 (0.450) | 0.264 (0.358) |
| Average *B*-factor (Å$^2$) | | | |
| Arl2 (no. of atoms) | 38.2 (1433) | 37.4 (1349) | 41.2 (1340) |
| PDEδ (no. of atoms) | 54.9 (1074) | 42.7 (1187) | 47.5 (1179) |
| Water (no. of molecules) | 40.2 (57) | 43.8 (126) | 54.4 (104) |
| GDP/Mg/$PO_4$ (occupancy) | – | 35.1/28.9/32.3 (1) | 38.1/29.9/54.4 (0.74) |
| GTP/Mg/water (occupancy) | 34.4/30.1/38.4 (1) | – | 16.9/29.9/61.7 (0.26) |
| R.m.s.d.[f] from ideal geometry | | | |
| Bond length (Å) | 0.010 | 0.007 | 0.007 |
| Bond angles (°) | 2.0 | 1.4 | 0.9 |
| Ramachandran plot[g] | | | |
| Most favored (%) | 84.4 | 90.5 | 90.5 |
| Disallowed (%) | 0.7 | 0.7 | 0.7 |

[a]Data collection statistics taken from Renault *et al*. (2001).
[b]Values in parentheses refer to the highest resolution shell.
[c]$R_{sym} = \Sigma_h\Sigma_i|I_{h,i} - \langle I_h\rangle|/\Sigma_h\Sigma_i I_{h,i}$
[d]$R_{work} = \Sigma_h|F_o - F_c|/\Sigma F_o$ (working set, no σ cut-off applied).
[e]$R_{free}$ is the same as $R_{cryst}$, but calculated on 10% of the data excluded from refinement.
[f]R.m.s.d. from target geometries.
[g]PROCHECK (CCP4, 1994).

α-helix with three turns. In its released conformation, this helix appears to be designed to interact with a membrane as observed with Arf proteins.

The binding of PDEδ was shown to strongly inhibit the dissociation of GTP from Arl (Linari *et al*., 1999). Although the structure of the uncomplexed Arl2-GTP is not available for comparison, we can see that the nucleotide is deeply buried in its canonical binding pocket and that the switch regions of Arl2 are fixed around it by PDEδ. We would assume that the mobility of the switch regions, which is at least partially responsible for nucleotide release (Vetter and Wittinghofer, 2001), is reduced in the complex and thus stabilizes nucleotide binding. It has also been noted that GTP hydrolysis is very slow with Arf/Arl proteins (Pasqualato *et al*., 2001). In the structure we see the crucial $Gln70_A$ pointing away from its position suitable for catalysis. There it would sterically clash with $Asp25_A$, located in the P-loop in a position that corresponds to Gly12 in Ras, the mutation of which blocks GTP hydrolysis.

### *PDEδ has a fold closely related to RhoGDI*

The structure of PDEδ (Figure 2A) features an immunoglobulin-like β-sandwich fold with two β-sheets that pack against each other. One is formed by strands β1, β2, β4 and β7, the other by β3, β5, β6, β8 and β9. This β-sandwich core domain is preceded by an N-terminal α-helix ($\alpha_1$) and shows only one further short $3_{10}$ helix in one of the loop regions. The loop connecting β7 and β8 is disordered, but present in the crystal as shown by mass spectrometry (see Materials and methods).

A search for structural relatives of PDEδ using the DALI server (Holm and Sander, 1996) produced 167 proteins, among which RhoGDI (Gosser *et al*., 1997; Keep *et al*., 1997) (Figure 2) stood out clearly as the best hit (*Z* score 9.8). This is all the more interesting as the 121 residues that are structurally aligned with an r.m.s.d. of 3.0 Å show a sequence identity of only 2%. RhoGDIs are able to extract C-terminally prenylated Rac, Rho and Cdc42 from cellular membranes. The resulting complexes thus constitute cytosolic pools of lipophilic Rho proteins

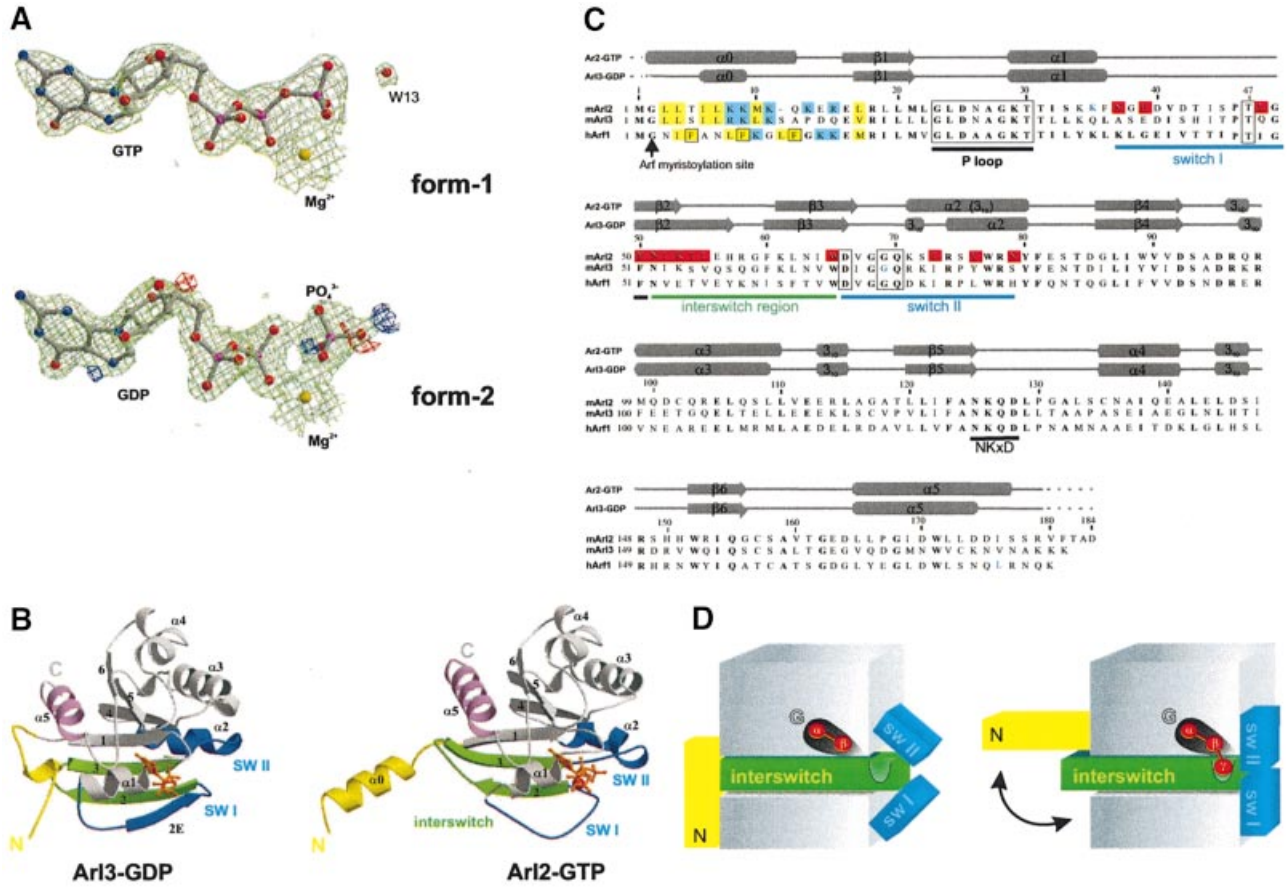


**Fig. 1.** The structure of Arl2-GTP. (**A**) Electron density maps around the bound nucleotide [$2F_o - F_c$ map contoured at 1.8σ (green), $F_o - F_c$ at 3σ (blue), and $F_o - F_c$ at –3σ (red)]. Upper panel: GTP, $Mg^{2+}$ (yellow sphere) and a water molecule (W13) in the active site of Arl2 in crystal form-1, at 2.3 Å resolution. Lower panel: GDP, phosphate and $Mg^{2+}$ in the active site of Arl2 in form-2, at 1.8 Å resolution. Note the positive difference density between the β phosphate and the phosphate ion, and, on the right, negative density at the phosphate ion and positive density for an additional water not added to the current model, indicating only partial hydrolysis and the presence of residual GTP/water. (**B**) Ribbon diagram of Arl3-GDP (with the additional β-strand $\beta_{2E}$) and Arl2-GTP (form-1), with switches in blue, interswitch region in green, N-terminus in yellow, C-terminal helix in magenta, nucleotides in orange and $Mg^{2+}$ as red sphere. (**C**) Sequence alignment of mmArl2, mmArl3 and hArf1. Contact sites between Arl2 and PDEδ are highlighted in red. Color coding in the amphipathic N-terminal region: hydrophobic residues in yellow, basic residues in blue. Phenylalanines characteristic for Arf proteins are boxed; conserved residues are in bold. Secondary structure elements were determined by PROCHECK (CCP4, 1994) (**D**) Schematic representation of the observed β register shift resulting in the release of the N-terminus. Color coding as in (B).

(Olofsson, 1999). The low sequence homology (Figure 2B) apparently prevented recognition of the close structural similarity that is now revealed by the crystal structure. While the overall β-sandwich fold of PDEδ and RhoGDI is identical, there are considerable differences in length and conformation of the loops. Moreover, the proteins show different N-terminal regions, with a 67-residue N-terminal extension preceding the immunoglobulin-like domain of RhoGDI, while only a short 14-residue α-helix is present in PDEδ. The N-terminal extension was not visible in the structures of free RhoGDI (Gosser *et al.*, 1997; Keep *et al.*, 1997).

### *The complex of Arl2-GTP and PDEδ*

The structure of the complex of Arl2-GTP and PDEδ is shown in Figure 3A. The interface is formed primarily by a parallel inter-protein β-sheet interaction involving β2 of the interswitch region of Arl2 and β7 of PDEδ, resulting in a 10-stranded β-sheet extending over both molecules. A similar, albeit anti-parallel, β-strand interaction has been observed in the complexes of Ras proteins with the Ras-binding domain of Raf (Nassar *et al.*, 1995) (Figure 3B) or RalGDS (Huang *et al.*, 1998; Vetter *et al.*, 1999) and PI3-kinase (Pacold *et al.*, 2000).

With RhoGDI being the closest structural relative of PDEδ, we compared Arl2-GTP:PDEδ with complexes of RhoGDIs and their targets (Hoffman *et al.*, 2000; Scheffzek *et al.*, 2000; Grizot *et al.*, 2001). Owing to the presence of an ordered geranylgeranyl moiety in the lipid binding pocket, we focused on the structure of Cdc42-GDP:RhoGDI1 (Hoffman *et al.*, 2000), which reveals a completely different interaction mode from that observed with Arl2-GTP:PDEδ, does not involve an inter-protein β-sheet and uses primarily switch II (Figure 3C). Instead of interacting only with the immunoglobulin-like domain, a major part of the interface and its specificity is mediated by the 58-residue N-terminal extension of RhoGDI. Except for two residues at the end of β6, there are no

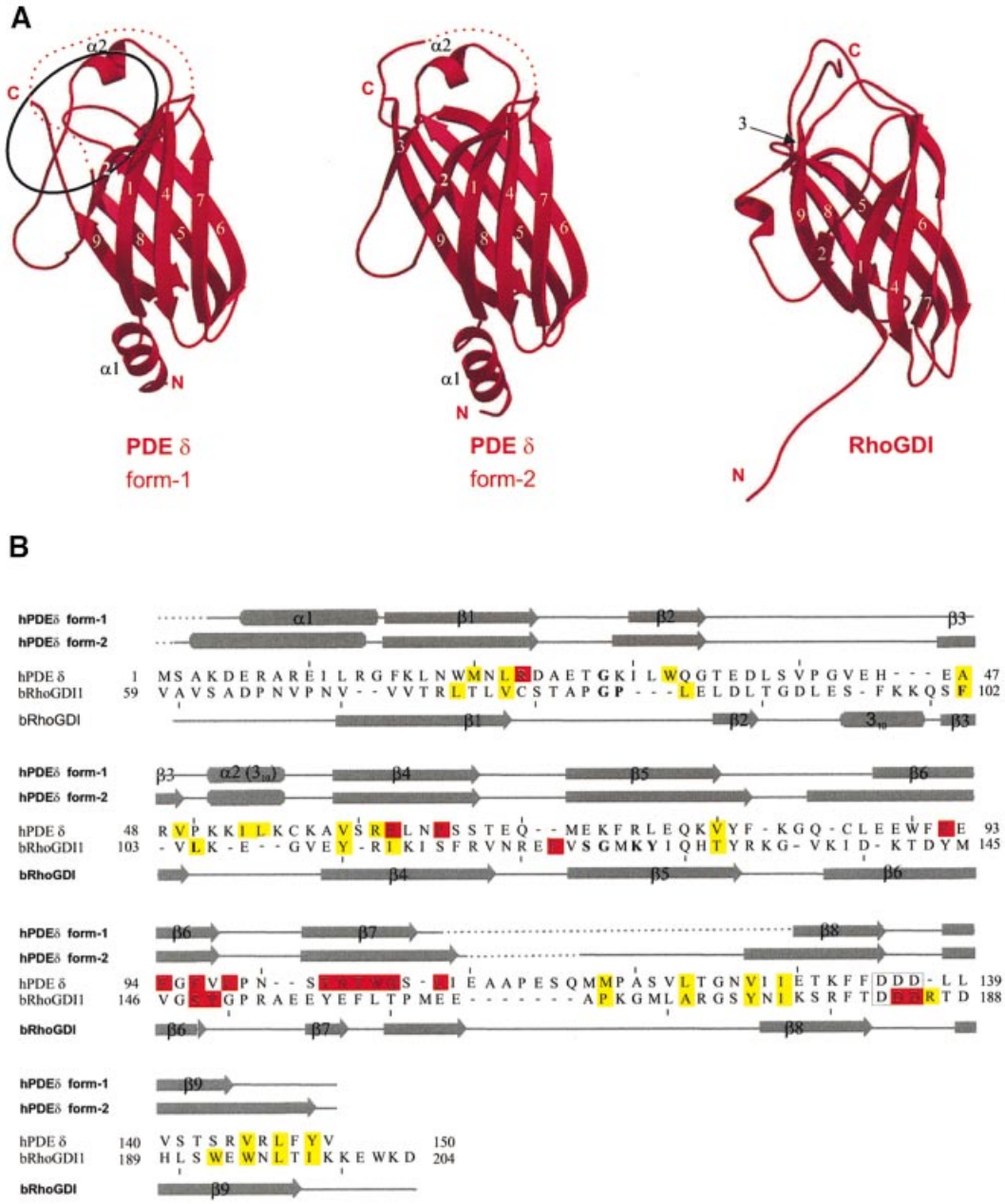


**Fig. 2.** The structure of PDEδ and comparison with RhoGDI. (**A**) Ribbon representations of PDEδ (crystal form-1 and -2) and RhoGDI (Gosser *et al.*, 1997). Disordered loops are shown as dotted lines. Note the degeneration of secondary structure and higher disorder in form-1, marked by an ellipse. (**B**) Structure based sequence alignment of full-length PDEδ (crystal form-2) and the C-terminal domain of RhoGDI1 (residues 59–204) produced with BRAGI (Schomburg and Reichelt, 1988). Highlighted in yellow are those residues of RhoGDI that contribute to the lipid binding pocket in the structure of Cdc42-GDP:RhoGDI (Hoffman *et al.*, 2000), and structurally equivalent residues that line the inner surface of the hydrophobic pocket of PDEδ. Residues contributing to the interface with Cdc42-GDP and Arl2, respectively, are highlighted in red.

overlaps between residues of RhoGDI interacting with Cdc42-GDP and those of PDEδ interacting with Arl2-GTP (Figure 2B), which further illustrates the different binding modes.

Figure 4 provides a detailed view into the interface of Arl2-GTP and PDEδ. There are eight main chain–main chain interactions between the two β-strands, many more than have been observed in the Ras:effector complexes. Interactions additional to the central β–β core involve residues from the switch regions of Arl2 and β6, β4, β1 and the β6/β7 loop from PDEδ. These residues show a remarkable distribution, with mostly hydrophobic interactions on one side and mostly polar interactions on the other side of the inter-protein β-sheet (Figure 4). This could suggest that the 'un-zipping' or a partial opening of the interface would be initiated on the hydrophilic side where water could access more easily. The large number of hydrophobic residues in the interface of PDEδ, which would be solvent-exposed in the absence of Arl2, explains the significantly improved bacterial expression of PDEδ achieved by co-expression with Arl2 (Renault *et al.*, 2001). The involvement of switch I, switch II and the

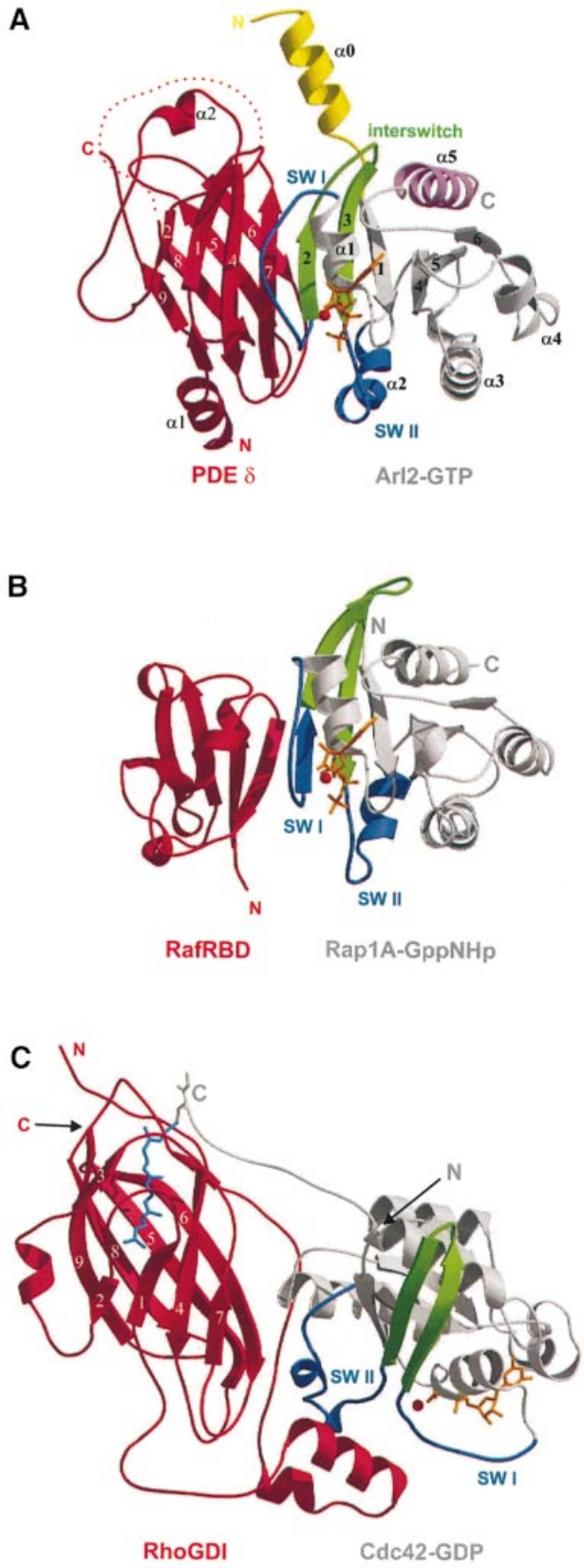


**Fig. 3.** Overall view of Arl2-GTP:PDEδ and comparison with Rap1A-GppNHp:RafRBD and Cdc42-GDP:RhoGDI. (**A**) Ribbon diagram of the complex of Arl2-GTP and PDEδ, with color coding of Arl2 as in Figure 1B. (**B**) Complex of Rap1A-GppNHp and the Ras binding domain of Raf (Nassar *et al*., 1995). Color coding as in (A). (**C**) Complex of Cdc42-GDP and RhoGDI1 (Hoffman *et al*., 2000). Color coding as in (A). C-terminal geranylgeranyl modification is shown in light blue.

interswitch region explains the specificity of PDEδ for the GTP-bound forms of Arl2 and Arl3 (Linari *et al*., 1999). Most of the observed interface residues would not be accessible in the GDP-bound state. In addition, we suggest that the specificity of PDEδ for Arl2/3 versus other Arf proteins is conveyed mainly by $Lys34_A$, $Glu39_A$ in switch I and $Lys53_A$ of the interswitch region. These three residues are located at or close to the interface with PDEδ and are highly conserved in all Arl2/3 orthologs, whereas they are very different in other Arf/Arl proteins. Interestingly, $Lys53_A$ also plays a critical role in $Mg^{2+}$ coordination in the GDP conformation (Hillig *et al*., 2000; Menetrey *et al*., 2000; Amor *et al*., 2001).

### *PDEδ features a hydrophobic pocket similar to RhoGDI*

The complex of Cdc42-GDP and RhoGDI (Figure 3C) shows that in addition to the interactions involving switch I and switch II, the C-terminus of Cdc42 folds into a shallow binding groove on top of the immunoglobulin domain. Also, its C-terminal geranylgeranyl moiety (shown in light blue in Figure 3C) inserts into a deep hydrophobic pocket formed between the two β-sheets of the β-sandwich. Surprisingly, a similar, but empty, hydrophobic pocket is present in the same position in PDEδ. The structure-based sequence alignment (Figure 2B) shows that the residues lining the inner surface of this hydrophobic pocket (highlighted in yellow in Figure 2B) are in identical or very similar positions in both proteins, suggesting that not only the fold but also the lipid binding pocket are common features of both PDEδ and RhoGDI. After superimposition of the protein backbone of RhoGDI and PDEδ, the geranylgeranyl moiety of Cdc42 fits surprisingly well over almost its complete length into the hydrophobic pocket of PDEδ (Figure 5). Minor steric clashes could be avoided by conformational changes of the side chains involved. Such an adaptation of the pocket in the presence of a lipid was also observed between the structures of free RhoGDI and RhoGDI in complex with prenylated Cdc42 (Gosser *et al*., 1997; Keep *et al*., 1997; Hoffman *et al*., 2000). A comparison of PDEδ in both crystal forms (Figure 2A) indicates that the disordered loop between β7 and β8, as well as a number of loops and secondary structure elements that are less well defined in form-1, are all located around this putative lipid binding pocket. This accumulation of disorder may be interpreted as a consequence of a missing lipid ligand that would stabilize this section of the protein.

### *Two-hybrid analysis reveals new binding partners of PDEδ*

From a number of observations we consider PDEδ to be an effector protein rather than a GDI for Arl2 and Arl3. The interface between Arl2 and PDEδ shows typical GNBP:effector interactions, the binding is specific for the GTP conformation and is tight in the absence of any lipid modification (Linari *et al*., 1999; M.Hanzal-Bayer, manuscript in preparation). In addition, binding to PDEδ does not require the N-terminal helix of Arl2 in qualitative two-hybrid experiments (data not shown). On the other hand, the overall GDI-like fold, as well as the presence of a hydrophobic pocket formed by residues homologous to those in RhoGDI, suggests that in addition to its role as an

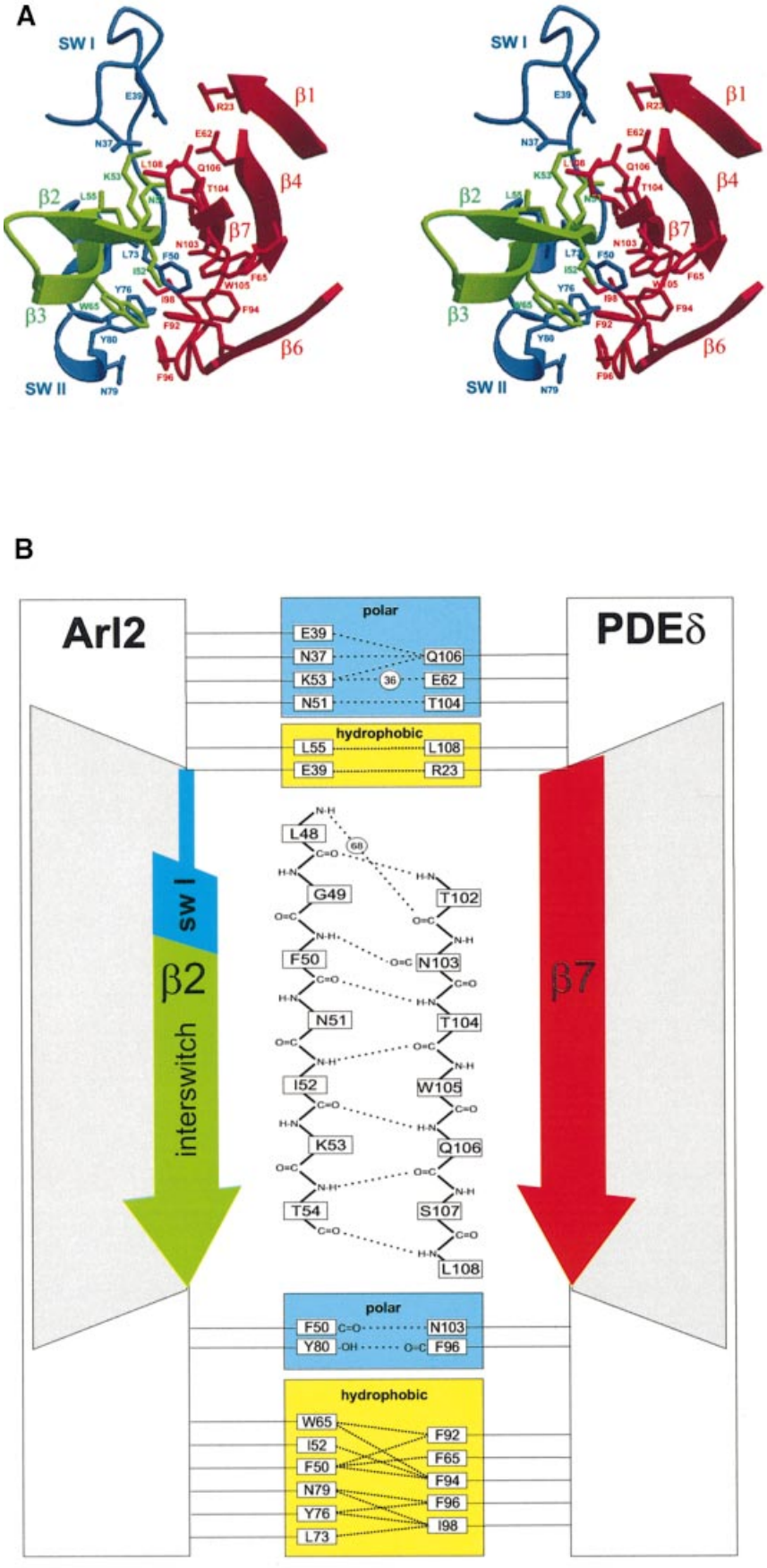


**Fig. 4.** The interface of Arl2 and PDEδ. (**A**) Stereo representation of a view along the β–β interface (Arl2-β2 and PDEδ-β7). (**B**) Schematic representation. Color coding as in Figure 3. Interactions as dotted lines. Residues are boxed, water molecules are represented by circles.

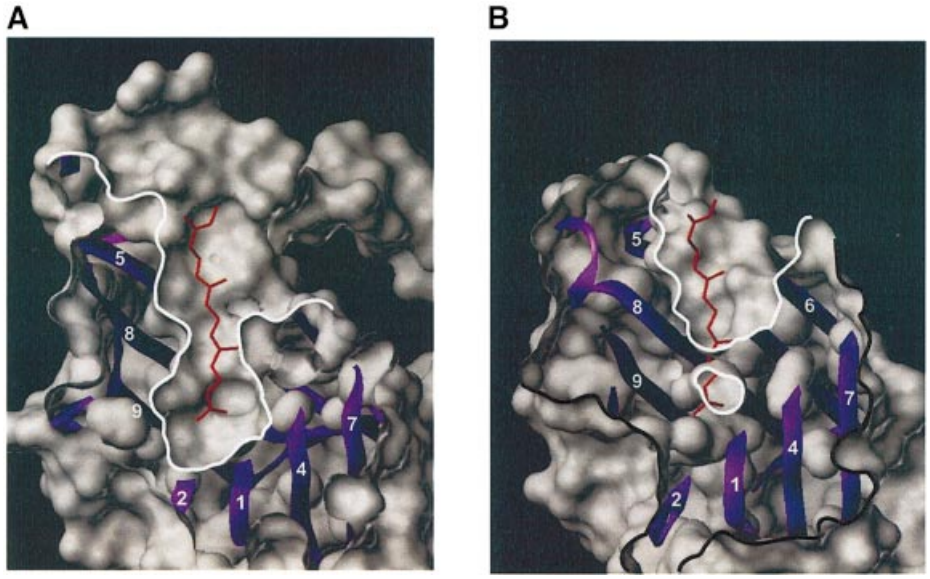


**Fig. 5.** The hydrophobic pocket in PDEδ. (**A**) Cut through a surface representation of RhoGDI showing the deep hydrophobic pocket with the geranylgeranyl moiety from the C-terminus of Cdc42-GDP (GDI is shown as a violet ribbon; geranylgeranyl moiety is shown in orange in stick representation). (**B**) PDEδ features a less deep but similarly hydrophobic pocket. The geranylgeranyl moiety of Cdc42 has been positioned by superimposition of the protein backbones of RhoGDI to PDEδ, followed by a small manual adjustment within the pocket. Full opening of the pocket would require only a small conformational change.

effector for Arl2 and Arl3, PDEδ is also an interacting protein for prenylated proteins, as suggested previously (Florio *et al*., 1996; Marzesco *et al*., 1998; Cook *et al*., 2000).

We therefore initiated a search for other targets of PDEδ's GDI-related function. As Rab13 has been found to interact with PDEδ (Marzesco *et al*., 1998), we used a number of available Ras-related GNBPs from various subfamilies and tested them by two-hybrid interaction assays. Assuming that the interaction of PDEδ with a target would depend on a prenylated C-terminus, we used full-length instead of CaaX box-deleted GNBPs, although this has previously been shown to interfere with the two-hybrid signal, presumably by interfering with localization in the nucleus. Of 22 GNBPs tested (Table II), H-Ras, Rheb, Rho6, $G\alpha_{i1}$ and possibly Rap1A interact with PDEδ with varying affinity in comparison with Arl2 and Arl3, which were used as positive controls (Figure 6A). Quantification of the affinities using the β-galactosidase assay (Figure 6B) is in good agreement with the qualitative growth data.

We had observed earlier for H-Ras and Raf-RBD that using full-length H-Ras results in a strong attenuation of the two-hybrid signal compared with using a C186S mutant, which cannot be processed. The simplest explanation for this is that full-length H-Ras inserts into membranes, which in turn keeps it from entering the nucleus. The strong signal observed with PDEδ suggests that it may prevent H-Ras from inserting into membranes. This is not due to an unspecific interaction of PDEδ with hydrophobic moieties, as 16 of the 22 GNBPs tested do not show any binding, although most of them have been shown to be myristoylated or prenylated (Table II). In addition, the affinities of the interacting proteins are clearly different.

### *Interaction of PDEδ with H-Ras requires an intact C-terminus*

To characterize further the interaction of PDEδ, we focused our attention on H-Ras and generated the mutants depicted in Figure 6C. Using the β-galactosidase assay, we found that truncation of the C-terminus of H-Ras (H-Ras 166) completely abrogates its interaction with PDEδ (note the logarithmic scale of the ordinate), clearly indicating that the C-terminus is absolutely required for binding. Secondly, as a Cys→Ser mutation of the farnesylation site (H-Ras C186S) in the full-length protein reduces galactosidase activity ~1000-fold, the post-translational modification of H-Ras is also required. Furthermore, the affinity is still higher than with H-Ras 166, which indicates that residues of the hypervariable region also contribute to the interaction. Finally, the affinity of PDEδ to H-Ras G12V is reduced ~7-fold compared with the wild type. This allows us to exclude the possibility that PDEδ is a previously unknown H-Ras effector, because in that scenario one would expect PDEδ to bind H-Ras G12V, which is predominantly in the GTP-bound state, with higher affinity than the wild-type, which is probably a mixture of both conformations. Instead, our result points to a preference of PDEδ for H-Ras-GDP over H-Ras-GTP, which is in agreement with observations made with RhoGDI (Michaelson *et al*., 2001).

## Discussion

The interaction of Arl2-GTP and PDEδ is strictly GTP dependent and involves the switch regions of the molecule, which is required for a bona fide effector. This is similar to the interaction of effector proteins with Ras, Rho and Ran, but completely different from the one observed between RhoGDI and Rho proteins. Since the binding is

**Table II.** List of GNBPs tested for interaction with PDEδ

| Protein | Organism | Interaction |
|---|---|---|
| Arf1 | *Homo sapiens* | – |
| Arf6 | *Homo sapiens* | – |
| Arl2 | *Mus musculus* | ++ |
| Arl3 | *Mus musculus* | +++ |
| Arl6 | *Homo sapiens* | – |
| Cdc42 | *Homo sapiens* | – |
| Rac1 | *Homo sapiens* | – |
| Rho6 | *Homo sapiens* | +++ |
| RhoC | *Homo sapiens* | – |
| Rab1 | *Canis familiaris* | – |
| Rab2 | *Canis familiaris* | – |
| Rab3a | *Bos taurus* | – |
| Rab7 | *Canis familiaris* | – |
| H-Ras | *Homo sapiens* | ++ |
| Rap1a | *Homo sapiens* | +/– |
| Rheb | *Rattus norvegicus* | + |
| Ral | *Saguinus oedipus* | – |
| Ran | *Homo sapiens* | – |
| $G\alpha_{i1}$ | *Rattus norvegicus* | + |
| $G\alpha_{t}$ | *Bos taurus* | – |
| GBP1 | *Homo sapiens* | – |
| Rad | *Homo sapiens* | – |

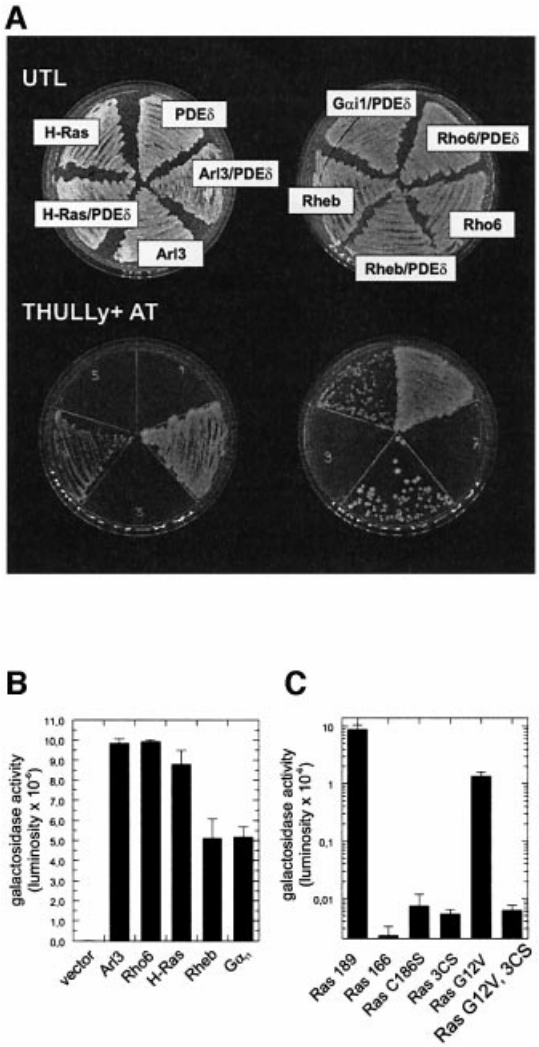


**Fig. 6.** Identification of new targets of PDEδ and initial characterization of the interaction between PDEδ and H-Ras. (**A**) Qualitative two-hybrid analysis. Growth data reveal H-Ras, Rheb, Rho6 and $G\alpha_{i1}$ as new interaction partners of PDEδ. (**B**) Quantitative β-galactosidase assay of the interactors shown in (A). (**C**) Quantitative β-galactosidase assay of PDEδ with the indicated mutant forms of H-Ras (3CS = C181S, C184S, C186S).

also independent of post-translational modifications, we conclude that PDEδ is an effector of Arl2 and the current structure thus represents the first structure of an Arf:effector complex.

The structure of PDEδ is closely related to RhoGDI and features a hydrophobic pocket similar to those found in RhoGDIs. It thus supplies a structural explanation for the ability of PDEδ to extract the catalytic subunits of PDE from the membrane and to constitute a cytosolic pool of the enzyme (Cook *et al*., 2001). A GDI-like function is also supported by the identification of the four new putative targets, H-Ras, Rheb, Rho6 and $G\alpha_{i1}$, that bind to PDEδ with varying affinities, together with the previously identified interaction with and solubilization of Rab13 (Marzesco *et al*., 1998). Supported by previous reports that PDEδ does not recognize prenylated rhodopsin kinase (Li and Baehr, 1998), Rab3a, Rab4, Rab6 or Rab8 (Marzesco *et al*., 1998), we can safely conclude that PDEδ binds to a number of C-terminally lipidated proteins by recognizing a specific binding motif around the prenylated cysteine that is presently undefined.

Although we can only speculate as to the nature of the Ras binding site of PDEδ, the major interaction sites observed in the complex of RhoGDIs with their target GNBPs are different in the Arl2-GTP:PDEδ complex, such that the binding sites are only partially overlapping (Figure 3A and C). Although the structure suggests that binding of farnesylated Ras should be different from the Rho:RhoGDI interaction in such a complex, the solvent-exposed N-terminal helix of PDEδ could, analogous to the N-terminal extension of RhoGDI, be involved. Close to this extension are three consecutive aspartate residues in loop β8/β9. They are involved in the interaction of RhoGDI with Cdc42 and, surprisingly, are conserved between PDEδ and all RhoGDIs. Finally, the hydrophobic pocket, after minor rearrangements also observed for RhoGDI, could accommodate the prenyl group.

Analogous to GDIs, PDEδ may function as a transport factor for H-Ras and other prenylated proteins, and release and/or the uptake would be mediated by Arl2/3. Release of other prenylated GNBPs from the corresponding GDI by suitable factors has been reported previously. It was demonstrated that target GNBPs complexed to their GDI in the GDP-bound form are not substrates of their cognate GEFs (Takai *et al*., 1995). Instead, GDI displacement factors (GDF) are needed to dissociate the GNBP from its GDI before activation can take place, and GDF proteins have been isolated for both RabGDI (Dirac-Svejstrup *et al*., 1997) and RhoGDI (Takahashi *et al*., 1997).

The proposed function of PDEδ would then be somewhat reminiscent of arfaptin/POR proteins that have been isolated as binders of both Rac1 and Arf proteins. Similar to our observations with PDEδ, arfaptins bind Rac1 independent of the nucleotide state, while their interaction with Arf1 or Arf6 is GTP specific (Tarricone *et al*., 2001).

Recently, Tarricone *et al*. (2001) provided a structural basis for the observed cross-talk between Rac1 and Arf proteins and suggested that arfaptin sequesters Rac1 until Arf-GTP binds to the same site and displaces it. Arfaptin would thus have a GDI-like function.

How does the observed Ras:Arl:PDEδ complex modify our thinking about Ras biology? Although much is known about the processing of Ras proteins (Gelb, 1997), and despite its implications for drug development, the transport of Ras proteins to the plasma membrane is still incompletely understood. There is evidence that H-Ras and N-Ras, but not K-Ras, are transported to the plasma membrane via the secretory pathway (Apolloni *et al*., 2000). Furthermore, it has been shown that a variety of membrane-anchored proteins are not uniformly distributed within the plasma membrane but instead are enriched in discrete microdomains referred to as caveolae and rafts (Simons and Toomre, 2000), and that H-Ras moves into and out of these caveolae, which is a regulated event required for proper function (Roy *et al*., 1999; Prior *et al*., 2001).

In conclusion, we would argue that the Arl2/3-regulated binding of PDEδ to prenylated proteins adds another level of complexity to the function of the latter. As a first alternative it could be envisioned that PDEδ is simply involved in the transport of H-Ras to the plasma membrane via secretory pathways. Alternatively, the interaction between PDEδ and farnesylated proteins may take place at the plasma membrane, where PDEδ may release proteins from irreversible membrane association for signaling purposes. Although a cytosolic pool of Ras proteins has never been observed, the complex might only be transient. It should also be noted that Rho6 (also referred to as Rnd1; Nobes *et al*., 1998), another tightly binding protein of PDEδ (Figure 6), is a Rho homolog that has no GTPase activity and is permanently in the activated state. The transient interaction with PDEδ, regulated by the Arl2/3 cycle, could thus in principle be a way of regulating Rho6. Future studies will have to be carried out to study different alternatives. The data presented should be valuable to guide such experiments.

## Materials and methods

### *Plasmid constructs*

Cloning of murine Arl2 and human PDEδ has been described previously (Renault *et al*., 2001). The open reading frames encoding the wild-type and full-length GNBPs listed in Table II were amplified by PCR, ligated into pBTM116 and verified by sequencing. Restriction sites were generated by PCR using appropriate primers. Rab cDNA was kindly provided by Kirill Alexandrov and Marino Zerial. Point mutants of H-Ras were generated using the QuikChange protocol (Stratagene).

### *Protein production, crystallization and data collection*

Full-length murine Arl2-GTP and human PDEδ were co-expressed in *E.coli* and the resulting complex was co-purified and crystallized in two crystal forms, as described previously (Renault *et al*., 2001). Due to cloning artefacts, Arl2 features the mutation S33L, and both proteins possess two additional N-terminal amino acids (Gly-Ser-). Rod-shaped crystals of form-1 grew within days and diffracted to 2.3 Å at ID13 (ESRF, Grenoble, France). More compact crystals of form-2 appeared after several months at 4°C. Here, a native data set to 1.8 Å and a SAD data set of the selenomethionine (SeMet)-labeled complex to 2.6 Å were collected at BW6 (DESY, Hamburg, Germany) and ID13 (ESRF, Grenoble, France; λ = 0.964 Å), respectively. A complete MAD data set could not be collected on the micro-focus beamline ID13, because SeMet-labeled crystals suitable for data collection grew very rarely and suffered highly from radiation damage during the data collection. Details of the data collections are given in (Renault *et al*., 2001) and are summarized in Table I.

### *Phasing, model building and refinement*

The structure was solved by a combination of Molecular Replacement and SAD phasing. Molecular Replacement (AMoRe; Navaza and Saludjian, 1997) was successful in both crystal forms (data sets Native-1 and SeMet) with both Arl3-GDP (Hillig *et al*., 2000) and Arf1Δ17-GppNHp (Goldberg, 1998) as search models, which was confirmed by clear density for three phosphates of the expected GTP (omitted from the search models). S.A.-composite omit maps (CNS 1.0; Brünger *et al*., 1998) allowed building of Arl2 (program O; Jones and Kjeldgaard, 1997). However, density for PDEδ remained very poor. Molecular replacement phases for both data sets were then significantly improved using ARP-wARP in mode 'molrep' (Perrakis *et al*., 1999). Although the resolution of data set SeMet was only 2.6 Å compared with 2.3 Å with Native-1, the quality of the density maps was better and the structure was first built using data set SeMet. The resulting $2F_o - F_c$-ARP maps allowed manual tracing of the first β-sheet of PDEδ (contacting Arl2-β2). After positional and grouped *B*-factor refinement (CNS), $R_{work}$ was at 0.441 ($R_{free}$ 0.489). Anomalous difference fourier maps (SeMet amplitudes/ARP phases) revealed four peaks higher than 4 σ, two coinciding with Arl2 $Met21_A$ and $Met99_A$, the other two later identified as PDEδ $Met20_P$ and $Met71_P$. SAD phasing, phase combination and solvent flattening (CNS) followed by iterative cycles of refinement and manual rebuilding allowed further tracing and correcting of the first sheet, plus eight residues of the N-terminal helix.

Independently of refinement and building with CNS/ARP, SHARP was used for refinement of the four SeMet sites and SAD phasing (Bricogne, 1997; de la Fortelle and Bricogne, 1997). Se occupancies were fixed to 1.0 and the f′ and f″ values refined. Hendrickson–Lattmann coefficients from this SHARP phasing were used throughout the refinement of an Arf1Δ17-GppNHp molecular replacement model using BUSTER-TNT (Bricogne, 1997). Manual rebuilding was alternated with cycles of maximum likelihood BUSTER-TNT refinement. During each round of refinement, scattering from the missing atoms was modeled with a low-resolution homographic exponential distribution, always based on the $2F_o - F_c$ density from the current phases (Roversi *et al*., 2000). Maximum entropy density modification was used at the end of each round of refinement to improve the density for those parts still missing.

This allowed initial tracing of 40 of the 152 residues of PDEδ: 33 residues of the first β-sheet and the N-terminal helix, plus seven residues of the second sheet that had not previously been built. SHARP/BUSTER and ARP/CNS were then used in parallel to gradually complete the second β-sheet and the connecting loops. At this point, a 1.8 Å resolution native data set for form-2 (Native-2) was collected, and refinement of form-2 was completed using these data. This revealed strong negative difference density between the β and γ phosphate, and GTP was therefore replaced by GDP and phosphate. The SAD heavy-atom phasing in SHARP was improved by addition of a third PDEδ SeMet site, three sulfur sites from the Arl cystein residues, and the GDP phosphor atoms, all of which were visible in the anomalous difference maps after solvent-flattening. Values for f′/f″ of the Se sites refined to –3.29/1.24 while values calculated with CrosSec (CCP4, 1994) are –3.5/3.72 respectively. Hendrickson–Lattmann coefficients from this SHARP refinement were used in the final BUSTER-TNT refinements.

The final model comprises Arl2 residues 15–179, PDEδ residues 2–150 (with 111–117 missing), GDP, one phosphate ion, two β-mercaptoethanol moieties and 126 water molecules ($R_{work}$ 0.244, $R_{free}$ 0.271; Table I). Two cysteines ($Cys135_A$ and $Cys86_P$) are modified by β-mercaptoethanol. $Cys86_P$ is involved in a crystal contact present in both forms and may thus have triggered re-crystallization.

Model building in form-1 was restarted with the refined model of form-2 as search model. Difference maps now clearly showed density for the N-terminal helix of Arl2. The final model comprises Arl2 residues 2–179, PDEδ residues 4–150 (with 109–129 missing), GTP, $Mg^{2+}$ and 57 water molecules ($R_{work}$ 0.255, $R_{free}$ 0.301). Finally, refinement against SeMet was completed using BUSTER-TNT. Here, both GDP/$PO_4$ and GTP/water were refined with occupancies of 0.74 and 0.26, respectively (see Table I for details). Superimpositions were produced with program O (Kleywegt and Jones, 1997) and BRAGI (Schomburg and Reichelt, 1988), figures with MOLSCRIPT (Kraulis, 1991), BOBSCRIPT (Esnouf, 1999), Raster3D (Merritt and Bacon, 1997) and Sybyl (Tripos, Inc.).

### Mass spectrometry

Thoroughly washed crystals were dissolved and analyzed by nano-electrospray mass spectrometry. Form-1 confirmed both full-length Arl2 and PDEδ (Renault *et al*., 2001). Form-2 revealed N-terminal degradation products of Arl2 ($Thr5_A$-$Asp184_A$ and $Met10_A$-$Asp184_A$) in addition to the full-length molecule ($Gly\text{-}Ser\text{-}Met1_A$-$Asp184_A$). For PDEδ, only full-length molecules were detected. Satellite peaks representing β-mercapto-ethanol-modified Arl2 and PDEδ confirmed the electron density peaks observed with form-2.

### HPLC analysis

The molar ratio of the nucleotides present in thoroughly washed crystals of form-2 was examined by isocratic HPLC (Beckman) on a C18 reversed-phase column (Ultrasphere; Beckman) under ion pair conditions in 100 mM potassium phosphate, 10 mM tetrabutyl ammoniumbromide and 5% (v/v) acetonitrile. Crystals used had been stored at 4°C for 18 months and contained GTP and GDP in a ratio of 0.45:0.55.

### Two-hybrid interaction assays

All interaction assays were done in the lexA-based two-hybrid system using the *S.cerevisiae* reporter strain L40 (Linari *et al*., 1999). In short, cells were transformed by the lithium-acetate method (Schiestl and Gietz, 1989) and grown at 30°C for a maximum of 4 days. Cells were selected for both plasmids on UTL plates (lacking leucine and tryptophan) and for interaction on THULLy plates (also lacking histidine). To suppress background growth, THULLy plates were supplemented with 25 mM of the inhibitor 3-aminotriazole.

### Quantitative two-hybrid assays

The activity of the β-galactosidase reporter was assayed using the GalactoStar system (Tropix; PE Biosystems). For each interaction four independent transformants were spread onto new agar plates, grown for 2 days at 30°C and resuspended in 20 ml liquid media. The $OD_{600}$ was determined twice, and equal cell numbers were harvested after transferring $3.6/OD_{600}$ ml to sterile tubes and adjusting the volume to 8 ml. Cells were resuspended in 800 µl Z-buffer [60 mM di-sodium hydrogenphosphate, 40 mM sodium-di-hydrogenphosphate, 10 mM potassium chloride, 1 mM magnesium sulfate (pH 7.0) 3.24 µl/ml mercaptoethanol], supplemented with 50 µl 0.1% (w/v) SDS, 50 µl chloroform and lysed for 30 s. Of the upper phase, 60 µl were mixed with 300 µl GalactoStar reagent, incubated on ice for 30 min, and luminosity was determined for a 5 s time interval in a Lumat LB9501 (Berthold). Each bar represents the arithmetic mean of 16 samples from four independent transformants, and it was ensured that all samples were incubated for exactly the same time.

### Co-ordinates

The co-ordinates and structure factors have been deposited with the Protein Data Bank (accession codes 1KSG, 1KSH and 1KSJ ).

## Acknowledgements

We would like to thank Gerard Bricogne for the use of a beta-version of the BUSTER program; Heino Prinz for mass spectrometry measurements; the Beamline staff at the micro-focus beamline ID13, ESRF Grenoble, and at the MPG/GBF wiggler beamline BW6/DORIS, DESY Hamburg, for access to synchrotron beam time and help during data collection; and Caroline Allen for critical reading of the manuscript. Data collection at ESRF was supported by the European Community Access to Research Infrastructures action of the Improving Human Potential Programme. We thank the EU for support (QLK3-CT-1999-00875).

## References

Amor,J.C., Harrison,D.H., Kahn,R.A. and Ringe,D. (1994) Structure of the human ADP-ribosylation factor 1 complexed with GDP. *Nature*, **372**, 704–708.

Amor,J.C., Horton,J.R., Zhu,X., Wang,Y., Sullards,C., Ringe,D., Cheng,X. and Kahn,R.A. (2001) Structures of yeast ARF2 and ARL1: distinct roles for the N terminus in the structure and function of ARF family GTPases. *J. Biol. Chem.*, **276**, 42477–42484.

Antonny,B., Beraud-Dufour,S., Chardin,P. and Chabre,M. (1997) N-terminal hydrophobic residues of the G-protein ADP-ribosylation factor-1 insert into membrane phospholipids upon GDP to GTP exchange. *Biochemistry*, **36**, 4675–4684.

Apolloni,A., Prior,I.A., Lindsay,M., Parton,R.G. and Hancock,J.F. (2000) H-ras but not K-ras traffics to the plasma membrane through the exocytic pathway. *Mol. Cell. Biol.*, **20**, 2475–2487.

Bhamidipati,A., Lewis,S.A. and Cowan,N.J. (2000) ADP ribosylation factor-like protein 2 (Arl2) regulates the interaction of tubulin-folding cofactor D with native tubulin. *J. Cell Biol.*, **149**, 1087–1096.

Bricogne,G. (1997) Bayesian statistical viewpoint on structure determination: basic concepts and examples. *Methods Enzymol.*, **276**, 361–423.

Brünger,A.T. *et al*. (1998) Crystallography & NMR system: A new software suite for macromolecular structure determination. *Acta Crystallogr. D*, **54**, 905–921.

Cavenagh,M.M. *et al*. (1994) ADP-ribosylation factor (ARF)-like 3, a new member of the ARF family of GTP-binding proteins cloned from human and rat tissues. *J. Biol. Chem.*, **269**, 18937–18942.

Chavrier,P. and Goud,B. (1999) The role of ARF and Rab GTPases in membrane transport. *Curr. Opin. Cell Biol.*, **11**, 466–475.

Collaborative Computational Project Number 4 (1994) The CCP4 suite: programs for protein crystallography. *Acta Crystallogr. D*, **50**, 760–763.

Cook,T.A., Ghomashchi,F., Gelb,M.H., Florio,S.K. and Beavo,J.A. (2000) Binding of the δ subunit to rod phosphodiesterase catalytic subunits requires methylated, prenylated C-termini of the catalytic subunits. *Biochemistry*, **39**, 13516–13523.

Cook,T.A., Ghomashchi,F., Gelb,M.H., Florio,S.K. and Beavo,J.A. (2001) The delta subunit of type 6 phosphodiesterase reduces light-induced cGMP hydrolysis in rod outer segments. *J. Biol. Chem.*, **276**, 5248–5255.

Cuvillier,A., Redon,F., Antoine,J.C., Chardin,P., DeVos,T. and Merlin,G. (2000) LdARL-3A, a *Leishmania promastigote*-specific ADP-ribosylation factor-like protein, is essential for flagellum integrity. *J. Cell Sci.*, **113**, 2065–2074.

de la Fortelle,E. and Bricogne,G. (1997) Maximum-likelihood heavy-atom parameter refinement for multiple isomorphous replacement and multiwavelength anomalous diffraction methods. *Methods Enzymol.*, **276**, 472–494.

Ding,M., Vitale,N., Tsai,S.C., Adamik,R., Moss,J. and Vaughan,M. (1996) Characterization of a GTPase-activating protein that stimulates GTP hydrolysis by both ADP-ribosylation factor (ARF) and ARF-like proteins. Comparison to the ARD1 gap domain. *J. Biol. Chem.*, **271**, 24005–24009.

Dirac-Svejstrup,A.B., Sumizawa,T. and Pfeffer,S.R. (1997) Identification of a GDI displacement factor that releases endosomal Rab GTPases from Rab-GDI. *EMBO J.*, **16**, 465–472.

Eboue,D., Icard-Liepkalns,C., Beringer,T.M. and Liepkalns,V.A. (1998) Attenuation of 19-9 antigen secretion in human colorectal carcinoma cell cultures by transfection with cDNA encoding novel ADP-ribosylation factor-like proteins. *Arch. Biochem. Biophys.*, **350**, 145–156.

Esnouf,R.M. (1999) Further additions to MolScript version 1.4, including reading and contouring of electron-density maps. *Acta Crystallogr. D*, **55**, 938–940.

Florio,S.K., Prusti,R.K. and Beavo,J.A. (1996) Solubilization of membrane-bound rod phosphodiesterase by the rod phospho-diesterase recombinant δ subunit. *J. Biol. Chem.*, **271**, 24036–24047.

Franco,M., Chardin,P., Chabre,M. and Paris,S. (1996) Myristoylation-facilitated binding of the G protein ARF1GDP to membrane phospholipids is required for its activation by a soluble nucleotide exchange factor. *J. Biol. Chem.*, **271**, 1573–1578.

Gelb,M.H. (1997) Protein prenylation, et cetera: signal transduction in two dimensions. *Science*, **275**, 1750–1751.

Gillespie,P.G., Prusti,R.K., Apel,E.D. and Beavo,J.A. (1989) A soluble form of bovine rod photoreceptor phosphodiesterase has a novel 15-kDa subunit. *J. Biol. Chem.*, **264**, 12187–12193.

Goldberg,J. (1998) Structural basis for activation of ARF GTPase: mechanisms of guanine nucleotide exchange and GTP-myristoyl switching. *Cell*, **95**, 237–248.

Gosser,Y.Q., Nomanbhoy,T.K., Aghazadeh,B., Manor,D., Combs,C., Cerione,R.A. and Rosen,M.K. (1997) C-terminal binding domain of Rho GDP-dissociation inhibitor directs N-terminal inhibitory peptide to GTPases. *Nature*, **387**, 814–819.

Greasley,S.E., Jhoti,H., Teahan,C., Solari,R., Fensome,A., Thomas, G.M.H., Cockcroft,S. and Bax,B. (1995) The structure of rat ADP ribosylation factor-1 (ARF 1) complexed to GDP determined from two different crystal forms. *Nature Struct. Biol.*, **2**, 797–806.

Grizot,S., Faure,J., Fieschi,F., Vignais,P.V., Dagher,M.C. and Pebay-Peyroula,E. (2001) Crystal structure of the Rac1–RhoGDI complex

involved in NADPH oxidase activation. *Biochemistry*, **40**, 10007–10013.
Herrmann,C., Martin,G.A. and Wittinghofer,A. (1995) Quantitative analysis of the complex between $p21^{ras}$ and the Ras-binding domain of the human Raf-1 protein kinase. *J. Biol. Chem.*, **270**, 2901–2905.
Hillig,R.C., Hanzal-Bayer,M., Linari,M., Becker,J., Wittinghofer,A. and Renault,L. (2000) Structural and biochemical properties show ARL3-GDP as a distinct GTP binding protein. *Structure*, **8**, 1239–1245.
Hoffman,G.R., Nassar,N. and Cerione,R.A. (2000) Structure of the Rho family GTP-binding protein Cdc42 in complex with the multifunctional regulator RhoGDI. *Cell*, **100**, 345–356.
Holm,L. and Sander,C. (1996) Mapping the protein universe. *Science*, **273**, 595–603.
Hong,J.X., Lee,F.J., Patton,W.A., Lin,C.Y., Moss,J. and Vaughan,M. (1998) Phospholipid- and GTP-dependent activation of cholera toxin and phospholipase D by human ADP-ribosylation factor-like protein 1 (HARL1). *J. Biol. Chem.*, **273**, 15872–15876.
Huang,L., Hofer,F., Martin,G.S. and Kim,S.H. (1998) Structural basis for the interaction of Ras with RalGDS. *Nature Struct. Biol.*, **5**, 422–426.
Jones,T.A. and Kjeldgaard,M. (1997) Electron-density map interpretation. *Methods Enzymol.*, **277**, 173–208.
Keep,N.H., Barnes,M., Barsukov,I., Badii,R., Lian,L.Y., Segal,A.W., Moody,P.C. and Roberts,G.C. (1997) A modulator of rho family G proteins, rhoGDI, binds these G proteins via an immunoglobulin-like domain and a flexible N-terminal arm. *Structure*, **5**, 623–633.
Kleywegt,G.J. and Jones,T.A. (1997) Model building and refinement practice. *Methods Enzymol.*, **277**, 208–230.
Kraulis,P.J. (1991) MOLSCRIPT: a program to produce both detailed and schematic plots of protein structures. *J. Appl. Crystallogr.*, **24**, 946–950.
Li,N. and Baehr,W. (1998) Expression and characterization of human PDEδ and its *Caenorhabditis elegans* ortholog CEδ. *FEBS Lett.*, **440**, 454–457.
Linari,M., Hanzal-Bayer,M. and Becker,J. (1999) The δ subunit of rod specific cyclic GMP phosphodiesterase, PDE δ, interacts with the Arf-like protein Arl3 in a GTP specific manner. *FEBS Lett.*, **458**, 55–59.
Lorenz,B., Migliaccio,C., Lichtner,P., Meyer,C., Strom,T.M., D'Urso,M., Becker,J., Ciccodicola,A. and Meitinger,T. (1998) Cloning and gene structure of the rod cGMP phosphodiesterase delta subunit gene (PDED) in man and mouse. *Eur. J. Hum. Genet.*, **6**, 283–290.
Marzesco,A.M., Galli,T., Louvard,D. and Zahraoui,A. (1998) The rod cGMP phosphodiesterase δ subunit dissociates the small GTPase Rab13 from membranes. *J. Biol. Chem.*, **273**, 22340–22345.
Menetrey,J., Macia,E., Pasqualato,S., Franco,M. and Cherfils,J. (2000) Structure of Arf6-GDP suggests a basis for guanine nucleotide exchange factor specificity. *Nature Struct. Biol.*, **7**, 466–469.
Merritt,E.A. and Bacon,D.J. (1997) Raster3D: photorealistic molecular graphics. *Methods Enzymol.*, **277**, 505–524.
Michaelson,D., Silletti,J., Murphy,G., D'Eustachio,P., Rush,M. and Philips,M.R. (2001) Differential localization of Rho GTPases in live cells: regulation by hypervariable regions and RhoGDI binding. *J. Cell Biol.*, **152**, 111–126.
Nassar,N., Horn,G., Herrmann,C., Scherer,A., McCormick,F. and Wittinghofer,A. (1995) The 2.2 Å crystal structure of the Ras-binding domain of the serine/threonine kinase c-Raf1 in complex with Rap1A and a GTP analogue. *Nature*, **375**, 554–560.
Navaza,J. and Saludjian,P. (1997) AMoRe: an automated molecular replacement package. *Methods Enzymol.*, **276**, 581–594.
Nobes,C.D., Lauritzen,I., Mattei,M.G., Paris,S., Hall,A. and Chardin,P. (1998) A new member of the Rho family, Rnd1, promotes disassembly of actin filament structures and loss of cell adhesion. *J. Cell Biol.*, **141**, 187–197.
Olofsson,B. (1999) Rho guanine dissociation inhibitors: pivotal molecules in cellular signalling. *Cell Signal.*, **11**, 545–554.
Pacold,M.E. *et al*. (2000) Crystal structure and functional analysis of Ras binding to its effector phosphoinositide 3-kinase γ. *Cell*, **103**, 931–943.
Pasqualato,S., Menetrey,J., Franco,M. and Cherfils,J. (2001) The structural GDP/GTP cycle of human Arf6. *EMBO rep.*, **2**, 234–238.
Perrakis,A., Morris,R. and Lamzin,V.S. (1999) Automated protein model building combined with iterative structure refinement. *Nature Struct. Biol.*, **6**, 458–463.
Prior,I.A., Harding,A., Yan,J., Sluimer,J., Parton,R.G. and Hancock,J.F. (2001) GTP-dependent segregation of H-ras from lipid rafts is required for biological activity. *Nature Cell Biol.*, **3**, 368–375.
Qin,N., Pittler,S.J. and Baehr,W. (1992) *In vitro* isoprenylation and membrane association of mouse rod photoreceptor cGMP phosphodiesterase α and β subunits expressed in bacteria. *J. Biol. Chem.*, **267**, 8458–8463.
Randazzo,P.A., Weiss,O. and Kahn,R.A. (1995) Preparation of recombinant ADP-ribosylation factor. *Methods Enzymol.*, **257**, 128–135.
Renault,L., Hanzal-Bayer,M. and Hillig,R.C. (2001) Coexpression, copurification, crystallization and preliminary X-ray analysis of a complex of ARL2-GTP and PDE delta. *Acta Crystallogr. D*, **57**, 1167–1170.
Roversi,P., Blanc,E., Vonrhein,C., Evans,G. and Bricogne,G. (2000) Modelling prior distributions of atoms for macromolecular refinement and completion. *Acta Crystallogr. D*, **56**, 1316–1323.
Roy,S., Luetterforst,R., Harding,A., Apolloni,A., Etheridge,M., Stang,E., Rolls,B., Hancock,J.F. and Parton,R.G. (1999) Dominant-negative caveolin inhibits H-Ras function by disrupting cholesterol-rich plasma membrane domains. *Nature Cell Biol.*, **1**, 98–105.
Scheffzek,K., Stephan,I., Jensen,O.N., Illenberger,D. and Gierschik,P. (2000) The Rac–RhoGDI complex and the structural basis for the regulation of Rho proteins by RhoGDI. *Nature Struct. Biol.*, **7**, 122–126.
Schiestl,R.H. and Gietz,R.D. (1989) High efficiency transformation of intact yeast cells using single stranded nucleic acids as a carrier. *Curr. Genet.*, **16**, 339–346.
Schomburg,D. and Reichelt,J. (1988) BRAGI: A comprehensive protein modelling program system. *J. Mol. Graph.*, **6**, 161–165.
Sharer,J.D. and Kahn,R.A. (1999) The ARF-like 2 (ARL2)-binding protein, BART—purification, cloning and initial characterization. *J. Biol. Chem.*, **274**, 27553–27561.
Simons,K. and Toomre,D. (2000) Lipid rafts and signal transduction. *Nature Rev. Mol. Cell. Biol.*, **1**, 31–39.
Takahashi,K., Sasaki,T., Mammoto,A., Takaishi,K., Kameyama,T., Tsukita,S. and Takai,Y. (1997) Direct interaction of the Rho GDP dissociation inhibitor with ezrin/radixin/moesin initiates the activation of the Rho small G protein. *J. Biol. Chem.*, **272**, 23371–23375.
Takai,Y., Sasaki,T., Tanaka,K. and Nakanishi,H. (1995) Rho as a regulator of the cytoskeleton. *Trends Biochem. Sci.*, **20**, 227–231.
Tamkun,J.W., Kahn,R.A., Kissinger,M., Brizuela,B.J., Rulka,C., Scott,M.P. and Kennison,J.A. (1991) The arflike gene encodes an essential GTP-binding protein in *Drosophila*. *Proc. Natl Acad. Sci. USA*, **88**, 3120–3124.
Tarricone,C., Xiao,B., Justin,N., Walker,P.A., Rittinger,K., Gamblin,S.J. and Smerdon,S.J. (2001) The structural basis of Arfaptin-mediated cross-talk between Rac and Arf signalling pathways. *Nature*, **411**, 215–219.
Vetter,I.R. and Wittinghofer,W. (2001) The guanine nucleotide-binding switch in three dimensions. *Science*, **294**, 1299–1304.
Vetter,I.R., Linnemann,T., Wohlgemuth,S., Geyer,M., Kalbitzer,H.R., Herrmann,C. and Wittinghofer,A. (1999) Structural and biochemical analysis of Ras-effector signaling via RalGDS. *FEBS Lett.*, **451**, 175–180.

*Received January 17, 2002; revised March 4, 2002; accepted March 5, 2002*